Toward Stealthy and Powerful Clean-label Backdoor Attacks via Trigger-specific Selection of Samples

Anonymous Author(s)
Affiliation
Address
email

Abstract

Backdoor attacks aim to covertly inject attacker-desired behavior into Deep Neural Networks (DNNs). Clean-label backdoor attacks are seen as the stealthiest attacks as adversaries can only poison samples from the target class without changing their labels. The effectiveness of clean-label attacks can be enhanced by carefully selecting poisoned samples. However, the collaborative effect of data poisoning selection and trigger design remains under-explored. In this paper, we highlight the significance of trigger-specific sample selection from two angles: boosting trigger stealthiness and efficiency. Firstly, we enhance the Bits Per Pixel (BPP) trigger by distinct color quantitation based on the human eyes' inherent poor insensitivity to blue light, and the invisibility of the trigger is ensured by poisoning the images with the smallest perceived distance changes during quantization. By poisoning 2.5% images of CIFAR10, the optimized attack overwhelms the BPP Attack by Attack Success Rate (ASR) from 12.5% to 68.89% even without label poisoning and training control. Secondly, we notice that current metrics ignore the competition between trigger features and non-target class robust features. For example, the forgetting-event metric only focuses on the frequency of forgetting events without paying attention to the category information of incorrect results. In sample selection, the consideration of category information for incorrect results varies across diverse triggers due to different extent of interference from non-target features on the learning of toxic features. Extensive experiments exhibit the tremendous superiority of trigger-specific metrics upon enhancing attacks across CIFAR10, CIFAR100, and Tiny-imagenet datasets.

Remark of poisoned samples generation The effectiveness of poison-only backdoor attacks hinges on the selection of poisoned data and the design of the trigger. However, **sample selection and trigger design of current methods are handled independently.** The goal of our paper is to find a simple but efficient poisoning sample selection strategy that can be generally applicable to various poison-only clean-label backdoor attacks by exploring the collaborative effect of step 1 and step 2.

1 Introduction

Deep neural networks (DNNs) have gained widespread adoption owing to their proven effectiveness and efficiency. However, their accuracy comes at the cost of intelligibility: it is usually unclear how they make their decisions (Radenovic et al. [2022]) and what they have learned, which poses significant challenges for scientists in efficiently defending the backdoor attacks (Doan et al. [2021],Lv et al. [2023], Zeng et al. [2023]). The deployment of models harboring security flaws pose a threat to the development of secure applications in important areas like finance, healthcare, Machine-Learning-as-a-Service (MLaaS)(Huang et al. [2024]), autonomous driving, and beyond, thus rendering the investigation of backdoor attacks a vital area of research endeavor.

Submitted to 38th Conference on Neural Information Processing Systems (NeurIPS 2024). Do not distribute.

Backdoor attacks aim to inject the behavior desired by the attacker into the model in a covert manner. A successful covert attack hinges on choosing a trigger pattern that remains effective at low poisoning rates while being stealthy to the human eye to evade manual inspections. Furthermore, most attacks can be set up as more challenging clean-label attack scenarios. Clean-label backdoor attacks ((Huynh et al. [2024], Zhao et al. [2024])) are seen as the stealthiest attacks as adversaries can only poison samples from the target class without changing their labels. However, current attacks confront challenges in achieving both potency and invisibility without label poisoning in a straightforward way. For example, Wang et al. [2022] proposed BppAttack, a stealthy attack which induces triggers based on image quantization and dithering. Due to the limited potency of imperceptible alterations, adversaries resort to adversarial training with label flipping to effectively embed the triggers. Generally speaking, BppAttack cannot achieve a powerful clean-label invisible backdoor attack by only poisoning the dataset.

Gao et al. [2023] reveals that the challenge of clean-label attacks primarily stems from the conflicting effects of 'robust features' associated with the target class within poisoned samples. Therefore, a simple yet effective plug-in method is proposed to enhance clean-label backdoor attacks by poisoning 'hard' instead of random samples. However, existing methods (Hayase and Oh [2022], Li et al. [2023b], Li et al. [2024b], Hung-Quang et al., Wang et al., Han et al. [2024]) overlook the stealthiness aspect of poisoned data selection and fail to consider the influence of non-target class robust features on trigger feature learning. The collaborative effect of data poisoning selection and trigger design remains under-explored. In this paper, we highlight the significance of trigger-specific sample selection in augmenting both trigger stealthiness and efficiency.

First of all, we demonstrate how to effectively and simply address the dilemma of the BppAttack by designing a trigger-specific sample selection strategy from the perspective of stealthiness. Computers represent image colors based on the three primary colors and BppAttack quantizes three colors uniformly (32:32:32), neglecting the differences in human visual perception and machine representation. For machine learning models, the data from these three color channels are treated equally during training. However, human perception exhibits marked differences in sensitivity to different colors. For example, humans exhibit limited sensitivity to blue light because the blue-sensitive cone cells comprises merely 5% in the human visual system. Land and McCann [1971] sets the ratio of RGB as 60:35:6 from the perspective of human perception. Therefore, we adjusted the quantization ratios of the three colors, with particular emphasis on increasing the poisoning intensity in the blue channel. It is worth noting that human eye's sensitivity to color perception is complex, with variations across different lighting scenarios and among individuals. Therefore, additional measures are still needed to ensure the invisibility of the trigger. The stealthiness of the optimized trigger, dubbed Multi-BPP, is assured in this paper by poisoning the images with the smallest perceived distance variations during quantization. Compared to BppAttack, Multi-BPP increases Attack Success Rate (ASR) from 12.5% to 68.89% with 2.5% poison rate in CIFAR10 without label flipping and training control in a straightforward approach.

Furthermore, trigger-specific sample selection demonstrates significant advantages in further enhancing the efficiency of backdoor attacks. Current trigger-uncoupled metrics (forgetting events, loss, and gradients) ignore the competition between trigger features and non-target class robust features. For example, current methods based on forgetting events (Gao et al. [2023]) only focuses on the frequency of forgetting events without paying attention to the category information of incorrect results. Extensive experiments on the CIFAR10, CIFAR100, and Tiny-ImageNet datasets indicate that the optimal balance between the diversity of jumped categories and the frequency of forgetting depends on the trigger pattern. Most triggers can be classified into two categories based on the size of the poisoning area. Backdoor attacks, represented by Badnets (Gu et al. [2017]), use visible embedding high-intensity features in a limited section of images as triggers. A small but high-intensity poisoning area allows the model to learn trigger features with minimal interference from global features (robust features of non-target classes) as models tend to take shortcuts during training. Alternatively, other attacks including blend (Chen et al. [2017]) enhance the stealthiness of the triggers while maintaining a high attack success rate by contaminating the entire image, which is the most classical trigger pattern having the widest room for design. The competition between trigger features and non-target class robust features matters when devising sample selection to enhance the efficiency of those triggers. For diverse triggers, the extent to which category information of incorrect results is considered varies in sample selection. Compared to existing trigger-decoupled methods, an apt trigger-specific sample selection can markedly enhance the attack success rate (ASR) of clean-label backdoor attacks.

The contributions of our paper are as follows:

- Compared to BppAttack (Wang et al. [2022]), the proposed Multi-BPP increases Attack Success Rate (ASR) from 12.5% to 68.89% with 2.5% poison rate in CIFAR10 without label flipping and training control by simply designing a trigger-specific sample selection strategy from the perspective of stealthiness.
- The trigger-specific metrics, optimized by accounting for the competition between trigger features and robust features of non-target classes, exhibit tremendous superiority in enhancing attacks across CIFAR10, CIFAR100, and Tiny-imagenet datasets. It is worth noting that, given that backdoor defense usually assumes that the poisonous features are the strongest features in the training data (Khaddaj et al. [2023]), attacks by poisoning the overall region gradually become the main research direction of backdoor attacks due to concealment and feature strength control. Therefore, robust features of non-target classes play an especially important role for most advanced attacks.
- The efficiency of poison-only attacks depends on the sample selection and the trigger pattern. However, the collaborative effect of data poisoning selection and trigger design remains under-explored. In our paper, extensive experiments demonstrate the value to construct stealthy and powerful clean-label backdoor attacks via trigger-specific selection of samples.

2 Related Work

Deep neural networks (DDNs) are vulnerable to backdoor attacks. The trojaned models function normally with regular inputs but misclassify to a target label with input stamped by the trigger (Gu et al. [2017], Chen et al. [2017]). At present, attackers have designed effective backdoor attacks in multimodal learning (Wang et al. [2024], Han et al. [2024]), federated learning (Li et al. [2023a], Chen et al. [2023]), diffusion model (Chou et al. [2023], Li et al. [2024a]), dataset distillation (Liu et al. [2023]) and other scenarios (Zhao et al. [2024]). Furthermore, attackers explore various ways to inject the desired behavior into DDNs. Bai et al. [2022] construct attack by manipulating model parameters (Qi et al. [2022]) via bit flipping. UBA-Inf (Huang et al. [2024]) activates a camouflaged backdoor through unlearning requests.

Despite the variety of application scenarios and triggering methods for backdoor attacks, mainstream research predominantly focuses on Computer Vision (CV), given its widespread use. Notably, data-poisoning backdoor attacks have attracted significant attention owing to their practicality. These attacks aim to embed backdoors into models by manipulating the training dataset, without controlling the training process of the target model. The effectiveness of a data poisoning attack depends on the design of the trigger and the selection of poisoned data. However, **current related research is conducted independently and the synergistic effect has not been adequately emphasized.**

2.1 Trigger Design

Traditional attacks (Gu et al. [2017], Chen et al. [2017]) utilize visible patch-based triggers (e.g., a square pattern), rendering them detectable by both humans and machines. The essence of advanced trigger design lies in identifying a stealthy feature that is conducive to machine learning.

In computer vision (CV) applications, the common strategy involves incorporating minor perturbations by tweaking the pixel values and positions of the original image (Bai et al. [2022]). Despite its inherent stealthiness, the constraint of invisibility poses a significant limitation and conflict in balancing attack efficiency and the utility of the poisoned model. Efforts to overcome these challenges frequently result in high injection rates, ineffective backdoor embeddings, limited transferability, and/or weakened robustness. For example, Wang et al. [2022] introduces BppAttack, a covert attack mechanism that leverages image quantization and dithering to induce triggers. Given the constrained effectiveness of imperceptible modifications, adversaries struggle to enhance the efficiency of attacks by employing adversarial training combined with label flipping.

To overcome the conflict between effectiveness and stealthiness, Gao et al. [2024] generates powerful and stealthy triggers by viewing trigger design as a bi-level optimization problem. Additionally, Wenger et al. [2022] introduces natural triggers based on the hypothesis that there may be naturally occurring physically colocated objects already present in popular datasets such as ImageNet. Further-

more, Lin et al. [2020] propose a Trojan trigger formulated from a combination of existing benign features to bypass the machine detection.

Summary Although designing a powerful trigger is essential, these methods often fail to benefit other backdoor attacks accordingly. It is not feasible to simply combine existing methods to design an effective sparse and invisible backdoor attack. In the clean-label setting, approaches that rely solely on complex trigger designs (Wang et al. [2024], Huynh et al. [2024]) to ensure attack effectiveness are gradually encountering bottlenecks. Therefore, **seeking breakthroughs from a holistic perspective of the attack is an important issue.**

2.2 Sample Selection

Lowering the percentage of poisoned samples is one of the most direct ways to increase the stealthiness of backdoor attacks. Clean-label backdoor attacks are seen as the stealthiest attacks as adversaries can only poison samples from the target class without changing their labels. The effectiveness of clean-label attacks can be enhanced by carefully selecting poisoned samples. Gao et al. [2023] reveals the varying importance of each poisoning sample and selects 'hard' samples based on three metrics (e.g., forgetting events, gradients, and loss). Han et al. [2024] further improves the efficiency of attacks based on optimized backdoor gradient-based score (BAGS). Moreover, Hayase and Oh [2022] poses sample selection as a bi-level optimization problem: construct strong poison examples that maximize the attack success rate (ASR). Furthermore, some scientists propose novel sample selection methods based on poisoning masks (Zhu et al. [2023]), confidence-based scoring (Wu et al. [2023]), and high-frequency energy (Xun et al. [2024]).

Summary Current research on sample selection focuses on designing new metrics or training derivations to construct data-efficiency attacks without recognizing the synergistic effect between triggers and sample selection. BppAttack draws our attention to the fact that there are few invisible attacks without training trigger generators. We demonstrate how to effectively overcome the dilemma of BppAttack based on a trigger-specific sample selection without extra training from the perspective of stealthiness. Meanwhile, current methods overlook the differential interference of category information under different trigger feature learning. Therefore, from the perspective of enhancing attack effectiveness, trigger-specific sample selection is a valuable research direction.

3 Methodology

3.1 Preliminaries

3.1.1 Model Training

The model output function of the image classification can be denoted by $f_\theta : X \to Y$, where $x \in X = \{0, 1, \ldots, 255\}^{C \times H \times W}$ represents an image domain, $Y = \{y_1, y_2, \ldots, y_k\}$ is a set of k classes, and θ denotes the parameters that a DNN learned form the begin training dataset $D_{tr} = \{(x_i, y_i)\}_{i=1}^{N}$.

The benign training with D_{tr} can be seen as a single-level optimization problem. The optimization seeks a model f_θ by solving the following problem during training:

$$\min_{\theta} L(D_{tr}, f_\theta) = \sum_{i=1}^{N_{tr}} l(x_i, y_i, f_\theta), \tag{1}$$

where l is the loss function (e.g., the cross-entropy), and $(x_i, y_i) \in D_{tr}$.

3.1.2 Poion-only Clean-label Backdoor Attacks

Attack Knowledge In a poison-only backdoor attack, an adversary has access to the original training dataset D_{tr} and is allowed to inject the pre-defined trigger into a small subset of the training set. Specifically, attacks can be called clean-label attacks if the adversary does not change the ground-truth label of the origin data. Furthermore, the adversary has no knowledge and the ability to modify other training components (e.g., loss functions, model architecture, training schedule,

optimization algorithm, etc). Hence, the attacker can not manipulate the model weights in any other way except by poisoning the dataset, and the latent connection between the trigger and the target label will be learned only during the training process. In the inference stage, we assume that the adversary is not able to access the prediction vectors. In general, poison-only clean-label attacks require minimal capacities and therefore can be applied in many real-world scenarios.

Attack Workflow The detailed workflow of a poison-only clean-label backdoor attack is presented to elaborate the theory of backdoor attacks. How to generate the poisoned dataset D_p is the cornerstone of the attack. We will remark on the important evaluation criteria in each step.

Step 1: Select samples to be poisoned (by attackers). D_p consists of two disjoint parts. Given a target label y_t, a subset D_s is selected from target-label set $D_t = \{(x_i, y_i)|(x_i, y_i) \in D_{tr}, y_i = y_t\}$ to be poisoned and the remain benign samples can be denoted as $D_b = D_{tr} \backslash D_s$. Here we define a binary vector $M = [M_1, M_2, \ldots, M_{|D_{tr}|}] \in \{0, 1\}^{|D|}$ to represent the poisoning selection. Specifically, $M_i = 1$ indicates that x_i is selected to be poisoned while $M_i = 0$ means the benign sample. We denote $\alpha := \frac{|D_s|}{|D_{tr}|}$ as the poisoning rate. Note that most existing backdoor backdoor attack methods randomly select $\alpha \cdot |D_{tr}|$ samples to be poisoned. α serves as a crucial indicator of stealthiness in poison-only attacks, facilitating their ability to evade both machine and manual inspections.

Step 2: Trigger Insertion (by attackers). In computer vision applications, the adversary designs a trigger pattern w by tweaking the pixel values and positions of the benign image. The generator of poisoned images can be denoted as $f_g : X \to X$. For example, $f_g(x) = (1 - m) * x + m * w$, where the mask $m \in [0, 1]^{C \times H \times W}$ representing the poison area of the trigger w and $*$ representing the element-wise product. Therefore, given the target label y_t in a clean-label attack, the generated poisoned training dataset could be denoted as $D_p = \{(x_i, y_i)|_{if\ m_i=0},\ or\ (f_g(x_i), y_t)|_{if\ m_i=1}\}_{i=1}^{|D_{tr}|}$. For stronger stealthiness, the attackers want the trigger w to be sufficiently invisible, which means the distance $L_D(f_g(x_i), x_i)$ should be small.

Step 3: Model Training (by users). Once the poisoned dataset D_p is generated, users will train the poisoned DNN via the period described in section 3.1.1. The stealthiness and utility of backdoor attacks require that the modification of the dataset should be unnoticeable to users, which means the poisoned model $\tilde{f}_\theta$ is expected to achieve high accuracy on benign test samples. Otherwise, users would not adopt the poisoned model and no backdoor could be implanted. The accuracy on clean test set D_{clean} can be computed by:

$$CleanACC = \frac{1}{N_{clean}} \sum_{i=1}^{N_{clean}} ACC(\tilde{f}_\theta(x_i), y_i) \tag{2}$$

where N_{clean} means the number of clean test set. $(x_i, y_i) \in D_{clean}$ and y_i is the ground-ruth label. $ACC(y_{pre}, y)$ will be set to 1 if $y_{pre} = y$ and 0 otherwise.

Step 4: Activate the backdoor using the trigger during the inference stage (by attackers). The attackers expect to activate the injected backdoor using the trigger w defined in step 2. Given the poisoned model $\tilde{f}_\theta$, the Attack Success Rate (ASR) of backdoor attack can be computed by:

$$ASR = \frac{1}{N_{clean}} \sum_{i=1}^{N_{clean}} ACC(\tilde{f}_\theta(f_g(x_i)), y_t) \tag{3}$$

where N_{clean} means the number of clean test set D_{clean}. $f_g(x_i)$ represents the poisoned image on image x_i and y_t is the target label. $\tilde{f}_\theta$ and $ACC(y_{pre}, y)$ are defined in Step 3.

3.2 Trigger-specific Selection Strategy

In this chapter, we present two simple yet effective approaches to enhance backdoor attacks by introducing trigger-specific selection strategies. In Section 3.2.1, we utilize the enhanced BppAttack (MultiAttack) as a prime example to demonstrate that a trigger-specific selection strategy from the standpoint of stealthiness can alleviate the constraints imposed on the backdoor features' invisibility. Therefore, we construact a more powerful attack. In Section 3.2.2, we delve into the intricate relationship between more refined data screening and the consideration of the poisoning area of the backdoor trigger Images with larger poisoning areas rely more on the assessment of non-target class

features in the filtering strategy. In the clean-label setting, samples that often shift across numerous categories carry more significance compared to those that only transition to a single class.

3.2.1 MultiBpp Attack

Multi-quantization Trigger BppAttack is a novel image color quantization based Trojan attack. Specifically, the attack first squeezes the benign color palette in each channel (e.g., m_b bits) of the image into a smaller color palette (m_p bits) by reducing the color depth. The squeezing function f_t of poisoning the image x can be defined in Eqn.4, where $round$ represents the integer rounding function:

$$f_t(x) = \frac{round(\frac{x}{2^{m_b}-1} * (2^{m_p}-1))}{2^{m_p}-1} * (2^{m_b}-1) \tag{4}$$

To further enhance the flexibility of the attack, MultiBpp refines the original quantization process for exploiting the differences between the human visual system and machine systems.: (1) We replace the color palette m_b, m_p in Eqn.4 by the number of representable colors N ($N_b = 2^{m_b}-1, N_p = 2^{m_p}-1$), which means that the poisoning intensity is more flexible and does not need to be a power of 2. Attackers can precisely control the strength of the poisonous features. (2) Based on the differences in human eye sensitivity to three color channels, we differentiate the poisoning intensity in the three color channels (e.g.,$N_b^c, N_p^c, c \in \{R, G, B\}$) instead of maintaining a uniform intensity (e.g.,N_b, N_p). The optimized equation can be represented as:

$$\tilde{f}_t^c(x) = \frac{round(\frac{x^c}{N_b^c} * (N_p^c))}{N_p^c} * (N_b^c) \tag{5}$$

To generate high-quality attack triggers, we also follow the previous method in BppAttack by introducing the Floyd-Steinberg dithering to enhance the trigger. Floyd-Steinberg dithering is an effective image dithering algorithm designed to achieve halftone effects in a limited color space. It employs an error diffusion strategy to reduce the visual impact caused by color reduction and produce a smoother image visually. It is worth noting that the quantization strength may vary during the error diffusion process, so the diffusion distribution $[d_1^c, d_2^c, d_3^c, d_4^c]$ need to be reasonably designed based on the quantization strength N_p^c. Details are presented in Algorithm 1.

Algorithm 1 Quantization with Floyd-Steinberg Dithering

Input : Selected Samples to be Poisoned D_s, Diffusion Distribution $[d_1^c, d_2^c, d_3^c, d_4^c]$
Output : Poisoned Samples
for image $x \in D_s$ **do**
  for $c \in \{R, G, B\}$ **do**
    for i from right to left **do**
      for j from top to bottom **do**
        $res^c = \tilde{f}_t^c(x^c[i][j]) - x^c[i][j]$
        $x^c[i][j] = x^c[i][j] + res^c$
        $x^c[i+1][j] = x^c[i][j] + res^c * d_1^c$
        $x^c[i+1][j+1] = x^c[i][j] + res^c * d_2^c$
        $x^c[i][j+1] = x^c[i][j] + res^c * d_3^c$
        $x^c[i-1][j+1] = x^c[i][j] + res^c * d_4^c$
      end for
    end for
  end for
end for

Metrics Optimized by Introducing Color Sensitivity The effectiveness of backdoor features conflicts with their stealthiness. we propose MultiBpp Attack to cleverly circumvent this conflict by incorporating the human visual system's preference for different colors. For example, Land and McCann [1971] sets the ratio of RGB as 60:35:6 from the perspective of human perception. By reinforcing the features in Eqn.5, especially when $c = b$, to varying degrees, we devise three trigger-specific select strategies to ensure the stealthiness of the backdoor trigger. $\tilde{F}_t^b$ represents the pixel variation function of MultiBpp attack. Firstly, we propose a simple strategy by only poisoning the pixels in the blue channel. In this case, it is reasonable to filter out the sample with the smallest

variations of pixels in the quantized blue channel given the poisoning rate α, which can be defined as

$$D_s = arg \max_{D_s \subset D_t} \sum_{(x_i,y_i)\in D_s} \sum_{h=1}^{H} \sum_{w=1}^{W} ||(\tilde{F_t^b}(x^b[h,w]) - x^b[h,w]||_2. \tag{6}$$

Secondly, the overall image's invisibility needs to be considered when poisoning covers all three color channels. We use SSIM (Structural Similarity Index Measure) to measure the structural similarity between the original image x and the poisoned image $\tilde{F}_t(x)$. The calculation formula of SSIM consists of three parts: 1. Luminance comparison $l(x, \tilde{F}_t(x))$, 2. Contrast comparison $c(x, \tilde{F}_t(x))$, 3. Structure comparison $s(x, \tilde{F}_t(x))$. Details can be denoted as

$$l(x, \tilde{F}_t(x)) = \frac{2\mu(x)\mu(\tilde{F}_t(x)) + C_1}{\mu(x)^2 + \mu(\tilde{F}_t(x))^2 + C_1}, \tag{7}$$

$$c(x, \tilde{F}_t(x)) = \frac{2\sigma(x)\sigma(\tilde{F}_t(x)) + C_2}{\sigma(x)^2 + \sigma(\tilde{F}_t(x))^2 + C_2}, \tag{8}$$

$$s(x, \tilde{F}_t(x)) = \frac{\sigma_{xy(x,\tilde{F}_t(x))} + C_3}{\sigma(x)\sigma(\tilde{F}_t(x)) + C_3}, \tag{9}$$

where $\mu(x)$ represents the mean of the image x, $\sigma(x)$ represents the standard deviation of the image x and $\sigma_{xy(x,y)}$ represents the covariance between image x and image y. C_1, C_2, C_3 are introduced to prevent division by zero errors. Therefore, we can calculate SSIM by introducing $[\beta_l, \beta_c, \beta_s]$ to control the weight of three considerations, which can be denoted in Eqn.10:

$$SSIM(x, \tilde{F}_t(x)) = [l(x, \tilde{F}_t(x))]^{\beta_l} * [c(x, \tilde{F}_t(x))]^{\beta_c} * [s(x, \tilde{F}_t(x))]^{\beta_s}, \tag{10}$$

However, SSIM overlooks human vision's differential sensitivity to color wavelengths. To address this, we perceptually reweight the weight of distance in different RGB channels based on human visual sensitivity curves by integrating the XYZ color space system in the International Commission on illumination (CIE-XYZ) , enabling prioritization of modifications in color regions least detectable to the human vision system. For convenience in expression, we use $\{R, G, B\}$ to represent value of pixels in the three color channels $\{x^R, x^G, x^B\}$. The core objective of the CIE-RGB system is to establish an anchored relationship between color and physical parameters, ensuring a one-to-one correspondence between color perception and tristimulus values. Its design focuses on color appearance through the proportioning of the three primary colors, rather than directly quantifying human eye sensitivity. The phenomenon that the human eye is most sensitive to green light (555nm) is reflected in the subsequent CIE-XYZ system through the luminance function $f_Y = 0.2126R + 0.7152G + 0.0722B$, but this weight distribution is a characteristic of the CIE-XYZ system, not the original design of the CIE-RGB system.

In 1931, CIE recommended conversion relationships between the two systems, primarily aimed at addressing the issue of negative values in the RGB system and ensuring that all tristimulus values in the new XYZ system are positive. Converting RGB values to CIE-XYZ tristimulus values follows a standardized process and the overall process of selecting samples can be outlined step-by-step below:

Step 1: Normalize CIE-RGB values. Step 1 aims to convert the value of image (R, G, B) to the range $[0, 1]$:

$$x^c_{norm} = \frac{x^c}{R + G + B}, c \in \{R, G, B\} \tag{11}$$

Specifically, we use $\{r, g, b\}$ to represent the normalized result $\{x^R_{norm}, x^G_{norm}, x^B_{norm}\}$.

Step 2: Convert normalized CIE-RGB to normalized CIE-XYZ. The conversion formulas of chromaticity coordinate conversion can be denoted as:

$$\begin{cases} X = (0.490r + 0.310g + 0.200b) \ / \ (0.607r + 1.132g + 1.200b) \\ Y = (0.117r + 0.812g + 0.010b) \ / \ (0.607r + 1.132g + 1.200b) \\ Z = (0.000r + 0.010g + 0.990b) \ / \ (0.607r + 1.132g + 1.200b) \end{cases} \tag{12}$$

Step 3: Calculate weights by CIE Standard Chroma Observer. CIE 1931 Standard Chroma Observer Spectral tristimulus Values, abbreviated as CIE Standard Chroma Observer, describes the

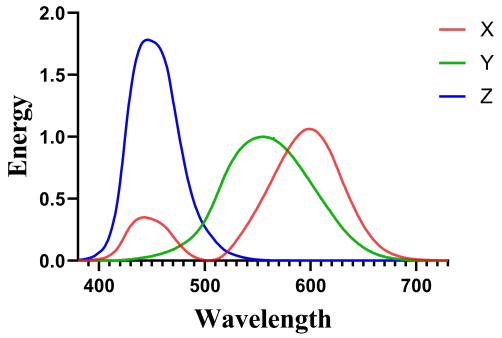

Figure 1: CIE 1931 Standard Chroma Observer Spectral tristimulus Values.

sensitivity of the human eye to light of different wavelengths. The curve at Figure 1 is plotted by artificial markers of which the stimulus values can be used to determine the weights in three channels.

Step 4: Sample selection by composite metric.

3.2.2 Metrics Optimized by Introducing Category Information

In this section, we will elaborate on how to reasonably adjust the filtering strategy by leveraging the size of the poisoning region in triggers, thereby selecting data that significantly increases the attack success rate. Compared to filtering from the perspective of stealthiness, a filtering strategy aimed at enhancing attack effectiveness requires a pre-training process. The core technique for sample selection is how to devise advanced metrics (i.e., Loss Value, Gradient Norm, and Forgetting Event) to evaluate the importance of samples for poisoning. Our methods are based on the observation and analysis of the drawbacks of current metrics.

Loss Value Given a benign model f_θ (trained on the benign training set D_{tr}), the loss value of model on sample (x_i, y_i) can be represented as $L(f_\theta(x_i), y_i)$. We choose samples with the greatest $\alpha * |D_{tr}|$ values in the subset D_t are chosen for poisoning:

$$D_s = arg \max_{D_s \subset D_t} \sum_{(x_i,y_i) \in D_s} L(f_\theta(x_i), y_i). \tag{13}$$

Gradient Norm Given a benign model f_θ (trained on the benign training set D_{tr}), the l_2- gradient norm of model on sample (x_i, y_i) can be represented as $||\nabla_\theta L(f_\theta(x_i), y_i)||_2$. We choose samples with the greatest $\alpha * |D_{tr}|$ values in the subset D_t are chosen for poisoning:

$$D_s = arg \max_{D_s \subset D_t} \sum_{(x_i,y_i) \in D_s} ||\nabla_\theta L(f_\theta(x_i), y_i)||_2. \tag{14}$$

Forgetting Event We name the event when a sample x_i was classified correctly in the previous epoch but incorrectly in the current epoch as a forgetting event of sample x_i. The number of forgetting events happened on sample x_i during the training process is denoted as $Num_{forget}(x_i)$. Those samples with the greatest $\alpha * |D_{tr}|$ forgetting statistics in the subset D_t are chosen for trigger injection:

$$D_s = arg \max_{D_s \subset D_t} \sum_{(x_i,y_i) \in D_s} Num_{forget}(x_i). \tag{15}$$

Remark The ultimate goal of proposing these selection criteria is to enhance the effectiveness of clean-label attacks. However, the actual definitions of these criteria do not establish a close connection with the clean-label setting. Additionally, ***these criteria are trigger-agnostic and fail to propose a simple but effective strategy to optimize the criteria based on the characteristics of the trigger.*** For example, the forgetting event criterion only selects data with high learning difficulty from dataset

D_{tr}, and its essence is unrelated to whether the attack is clean-label or dirty-label. What is more, samples are selected independently in the traditional selection strategy. For example, given a subset $D_{\tilde{s}}$ has been selected for poisoning, the selection of samples $D_s \backslash D_{\tilde{s}}$ will not be influenced by the already selected samples $D_{\tilde{s}}$. However, ***a more effective approach is to seek an overall optimal set rather than a simple combination of individually optimal ones.***

Our metric In the clean-label setting, we believe that data that frequently misclassifies to more classes are more valuable than data that frequently misclassifies to specific classes. Data that frequently misclassifies to more classes can, to some extent, represent data from different classes in a dirty-label scenario, thus bridging the gap between clean-label and dirty-label attacks. It is worth noting that we do not limit the value only to the categories to which the data shifts when a forgetting event occurs. Specifically, we record the distribution of all the categories y_e $(y_e \neq y_i)$ when the sample (x_i, y_i) is misclassified during the pre-training process. $N_e(y_m, (x_i, y_i))$ represents the number of times sample (x_i, y_i) is misclassified as y_m $(y_m \in Y \ and \ y_m \neq y_i)$. Our principle for designing metrics consists of several parts and thus our design of sample selection strategy can be regarded as a multi-level optimization problem.

Principle 1: Select hard samples. The first design principle aligns with the current mainstream selection principle, which is to identify and poison data that is more difficult to train. Unlike forgetting events, we relax some constraints. We believe that sample that is frequently misclassified is just as difficult to learn as data that often experiences forgetting events. The number of misclassification events (e.g., events that be misclassified as y_m $(y_m \neq y_i)$) that happened on sample (x_i, y_i) during the training process is denoted as $Num_e(x_i)$ $(Ne((x_i, y_i), y_m))$. Those samples with the greatest $\alpha * |D_{tr}|$ misclassification statistics in the subset D_t should enjoy prior selection for trigger injection:

$$D_s = arg \max_{D_s \subset D_t} \sum_{(x_i, y_i) \in D_s} Ne((x_i, y_i), y_m). \tag{16}$$

Principle 2: Ensure category diversity. The second design principle is to select samples D_s that cover more classes of the training set D_{tr} as much as possible. Consequently, the selected set D_s exhibits higher similarity and more robust coupling with the features of non-target classes, thereby rendering it challenging for the model to accurately classify D_s as the intended target class y_t. Therefore, the model is more likely to learn the strong correspondence between the features of the injected trigger and the target label y_t to enhance the effectiveness of the backdoor attack. We use $Exists(N_e((x_i, y_i), y_m))$ to represent whether there is a misclassification event that the model misclassify the x_i as y_m $(y_m \neq y_i)$ during the training process when function $Exists(N_e((x_i, y_i), y_m))$ output 1 and 0 otherwise. Those samples with the greatest $\alpha * |D_{tr}|$ statistics in the subset D_t should enjoy prior selection for trigger injection:

$$D_s = arg \max_{D_s \subset D_t} \sum_{(x_i, y_i) \in D_s} Exists(N_e((x_i, y_i), y_m)). \tag{17}$$

Principle 3: Ensure the balance in category proportions. The last design principle is to ensure that each category occupies a significant proportion in the filtered samples D_s. In the training dataset, there exist variations in the degree of similarity among diverse categories. For instance, the resemblance among animal classifications exceeds that among plant categories. Consequently, when a particular animal serves as the target label y_t, the volume of data erroneously labeled as plants during the pre-training phase will decline notably in comparison to data misidentified as other animals. According to the **Principle 1**, the image set that resembles the samples whose labels have low similarity with the target label will be difficult to select, thus weakening the consideration in **Principle 2**. The specific set that the model misclassifies as labels with minimal similarity to the intended target label y_t poses a greater challenge for the model to accurately classify within the target category. This difficulty makes it easier for the model to establish a strong connection between the backdoor trigger features and the target label y_t, thereby increasing the effectiveness of the attack. We use μ to represent the mean of $\{Ne((x_i, y_i), y_m)(y_m \neq y_t)\}$. The subset D_t including $\alpha * |D_{tr}|$ is expected to cover all categories in relatively balanced proportions:

$$D_s = arg \min_{D_s \subset D_t} \sum_{(x_i, y_i) \in D_s} ||N_e((x_i, y_i), y_m) - \mu||_2. \tag{18}$$

Implementation The aforementioned principles exhibit a degree of conflict with each other. Determining the appropriate magnitude of adjustment for the decision-making weights of these principles is of paramount importance. Our extensive experimental analysis has revealed that the allocation of these weights is contingent upon the coupling degree between trigger feature learning and non-target class features. In this paper, we propose a simple yet effective guidance method. Triggers with larger poisoning areas rely more on Principle 2 and Principle 3 than those triggers with smaller backdoor areas. We devise distinct negative functions N_F to facilitate the reduction of weights at varied rates (e.g.,$O(\log(n)), O(n), O(n^2)),\ and\ O(e^n)$) based on their relative proportions $n = \frac{Ne((x_i,y_i),y_m)}{\sum_{y_j \neq y_t} Ne((x_i,y_i),y_j)}(y_m \neq y_t)$. A strategy with a gradual weight reduction emphasizes **Principle 1**, whereas a rapid reduction favors **Principle 2** and **Principle 3**. What is more, we also propose a strategy, dubbed forget, to only consider **Principle 1**, and a strategy, dubbed num, to only consider **Principle 2**. Details are presented in Algorithm 2-5.

Algorithm 2 Metric Calculation with Negative Function N_F at $O(\log(n))$

Input : Train Dataset D_{tr}, Target Label y_t, Misclassification Events $N_e((x_i, y_i), y_m)$
Output : Calculated Metric of Samples
for image $(x_i, y_t) \in D_{tr}$ **do**
  $Num[y_m] = 0$
  for $y_m \in Y$ **do**
    $Num[y_m] = Num[y_m] + N_e((x_i, y_t), y_m)$
  end for
end for
for $y_m \in Y$ **do**
  $Sum = Sum + log(1 + Num[y_m])$
end for
for $y_m \in Y$ **do**
  $Cls[y_m] = 1 - \frac{log(1+Num[y_m])}{Sum}$
end for
for image $(x_i, y_t) \in D_{tr}$ **do**
  $Metric[x_i] = 0$
  for $y_m \in Y$ **do**
    $Metric[x_i] = Metric[x_i] + Cls[y_m] * N_e((x_i, y_t), y_m)$
  end for
end for

4 Experiments

4.1 Main settings

Dataset and Model. To clearly demonstrate the impact of category count on trigger feature learning across different poisoning regions, we conduct a series of systematic modifications to the CIFAR-100 dataset. Specifically, we meticulously select subsets with varying numbers of categories from CIFAR-100 for our experiments, terming these subsets CIFARX-N ($N \in \{10, 20, \ldots, 100\}$).

Baseline Selection. Compared to the aforementioned visible attacks, we also introduce BppAttack as a benchmark characterized by enhanced visual covertness but increased training complexity. BppAttack utilizes image quantization as the trigger feature and requires a higher poisoning rate, adversarial training, and label flipping to maintain effective attack performance. BppAttack employs image quantization as its trigger feature and necessitates a higher poisoning rate, adversarial training, and label flipping to sustain effective attack efficacy. Its primary advantage is its ability to maintain stealthiness by incorporating smoother and more difficult-to-detect perturbations without the need for training a trigger generator.

Attack Setup on CIFARX. For BadNets, a 33 checkerboard pattern is utilized as the trigger. For the Blended attack, a Hello-Kitty image is selected as the trigger and blended with the original images, with a transparency parameter of 0.2. Across all these attacks, 10% of the samples from the target class (representing 1% of the total samples) are poisoned, with the first class ("airplane") designated as the target class.

4.2 Superiority of MultiBpp Attack

4.2.1 Attack Setup.

To objectively describe the superiority of MultiBpp, we adopt the same experimental setup as BppAttack (Wang et al. [2022]). Specifically, the default bit depth of BppAttack in the original work is 5, which can be seen as $32:32:32$ in quantization. We use Base to represent the attack by quantizing the images with $32:32:32$ without any other process. Furthermore, we introduce the clean-label variants of Blend (dubbed 'Blend-C') to elaborate on the efficiency of the MultiBpp attack. For the Blended attack, a Hello-Kitty image is selected as the trigger and blended with the original images, with a transparency parameter of 0.2. Drawing upon the two strategies outlined in Section 3.2.1 for selecting poisoning data based on stealthiness, we devise two corresponding MultiBpp triggers. One involves poisoning exclusively the blue channel, which exhibits lower sensitivity to human perception, whereas the other implements differential poisoning across all channels. The quantization setting of poisoning intensity in RGB channels is approximately designed as $3:6:1$ according to the contribution to the brightness of images. (todo. poisoned images)

The first class ("airplane") is designated as the target class. The BppAttack gets a poor attack success rate (12.5%) with 2.5% samples poisoned upon CIFAR10 (Krizhevsky et al. [2009]) using Resnet18 (He et al. [2016]) and 2.5% is selected as the poisoning rate to construct all attacks. We assess all backdoor attacks using two classification metrics: CleanACC and ASR, which are denoted at **Section 3.1.2**. CleanACC (dubbed 'BA') represents the average prediction accuracy of all clean testing samples over 20 epochs, whereas ASR represents the average accuracy of their poisoned counterparts over 20 epochs. The objective of adversaries is to ensure attack effectiveness, characterized by a high ASR, while preserving the model's standard functionality, indicated by a high BA.

4.2.2 Result Analysis.

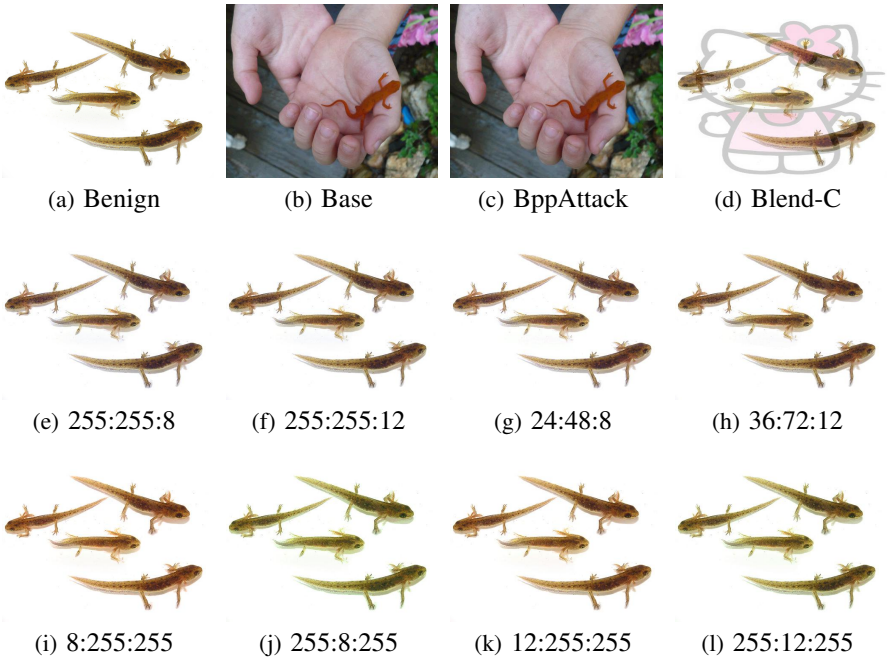

(a) Benign (b) Base (c) BppAttack (d) Blend-C

(e) 255:255:8 (f) 255:255:12 (g) 24:48:8 (h) 36:72:12

(i) 8:255:255 (j) 255:8:255 (k) 12:255:255 (l) 255:12:255

Figure 2: Images poisoned by different attacks. The images in the CIFAR-10 dataset have relatively low pixel quality, making it difficult to compare the subtle differences in visibility among different methods. Therefore, we have selected images from the training set of the same category in the ImageNet dataset, which has higher quality, as demonstrations. Methods a-d involve randomly selecting poisoned data, while methods e-l involve selecting images that are more concealed after poisoning.

Stealthiness The original BppAttack randomly selects data for poisoning. To maintain the stealthiness of the trigger, BppAttack needs to adopt a smaller quantization step $(32 : 32 : 32)$, which makes it difficult for the trigger features to be learned. Our method further optimizes based on two observations: 1. Images e, i, and j at Figure 2 correspond to the effects of poisoning the blue, red, and green channels, respectively. From a comparison of human visibility, it can be seen that the human eye is much less sensitive to the blue channel than to the other channels. Therefore, increasing the poisoning intensity in the blue channel can still maintain invisibility to the human eye. 2. According to Figure 2, images a and b show that within the same category of the same dataset, there are images with vastly different sensitivities to trigger features from a visibility perspective. By reasonably selecting data, the stealthiness of the trigger can be well ensured. The comparison between images d and b indicates that data that is insensitive to MultiBpp in terms of human visibility is more sensitive to Blend attacks. Moreover, performing a Blend attack based on image b will provide better concealment compared to attack based on image d. Therefore, The strategy for selecting insensitive data from the perspective of stealthiness still needs to consider the trigger features.

Attack			*Metric*		*Attack Setting*		
Type	no.	Method	BA(avg)	ASR(avg)	Clean-label	Training Control	Stealthy
Benchmark	a	Benign	-	**95.0%**	✓	✗	✓
	b	Base	**8.2%**	94.8%	✓	✗	✓
	c	BppAttack	**12.5%**	94.5%	✗	✓	✓
	d	Blend-C	**66.4%**	94.3%	✓	✗	✗
MultiBpp	e	255:255:8	68.6%	94.8%	✓	✗	✓
	f	255:255:12	60.0%	**94.9%**	✓	✗	✓
	g	24:48:8	**76.6%**	94.7%	✓	✗	✓
	h	36:72:12	57.7%	94.6%	✓	✗	✓
MultiBpp (others)	i	8:255:255	**84.1%**	**94.7%**	✓	✗	✗
	j	255:8:255	72.2%	94.3%	✓	✗	✗
	k	12:255:255	67.6%	94.5%	✓	✗	✗
	l	255:12:255	73.8%	94.5%	✓	✗	✗

Table 1: Performance of attacks by poisoning 2.5% samples of CIFAR10. **Red** represents the negative performance and requirement of attacks. $N_p^R : N_p^G : N_p^B$ in **Method** of MultiBpp represents the concrete quantization setting of poisoning intensity in RGB channels. Furthermore, Bengin serves as the original training period without being poisoned by backdoor attacks.

Attack Performance According to Tables 1c and 1b, even under strong conditions such as label flipping and controlled training, BppAttack still cannot guarantee the effectiveness of the attack (ASR of 12.5%) at a poisoning rate of 2.5%. As shown in Tables e-h, our proposed method significantly improves the attack effect under the clean-label setting and with only the dataset being poisoned. Specifically, MultiBpp achieves an ASR of 76.6% with a quantization step of 24:48:8 while maintaining a higher BA. Furthermore, Tables 1i-l indicate that there are still differences in efficiency when poisoning different channels. Specifically, poisoning the red and green channels yields better results. We speculate that the model also infers during the learning process that features in the red and green channels are more valuable, leading to different learning sensitivities. Tables 1e and f, as well as g and h, both indicate that increasing the quantization step generally improves the attack success rate. It is worth noting that a comparison between f and h suggests that there are exceptions to this rule. We speculate that the learning effectiveness of poisoning features is not solely influenced by the intensity of quantization efforts. Specifically, in scenarios with lower quantization intensity (f and h), the model needs to focus on features from three channels when learning h, whereas it only needs to attend to features from one channel when learning f. In such scenarios, the model finds it easier to learn f rather than h, which involves a greater quantization effort.

4.3 Superity of Trigger-specific Selection(todo name)

4.3.1 Attack Setup.

We conduct experiments on two benchmark datasets, including CIFAR-10 and CIFAR-100 (Krizhevsky et al. [2009]), with ResNet-18 (He et al. [2016]). We compare our plug-in methods against the standard version with random selection (dubbed 'vanilla') and existing sample selection strategies based on various metrics (such as forgetting events, gradient norm, and loss value). To ob-

jectively describe the superiority of our method, we adopt the same experimental setup as the setting devised by Gao et al. [2023]. We introduce the clean-label variants of two classic poisoned-label attacks: BadNets (dubbed 'BadNets-C') as a representative of attacks with small poisoning area, and an attack utilizing a blended strategy (dubbed 'Blended-C') as a representative of attacks poisoning the whole image, by poisoning samples only from the target class. For BadNets, a 3×3 checkerboard pattern is utilized as the trigger. For the Blended attack, a Hello-Kitty image is selected as the trigger and blended with the original images, with a transparency parameter of 0.2. Considering that the main objective of this chapter is to demonstrate the superiority of the filtering strategy in enhancing attack effectiveness, the selection of poisoned data for the MultiBpp attack in this chapter will be entirely consistent with that of other attacks. The stealthiness of the trigger is ensured by the quantization strength. In CIFAR10, we adopt the more stealthy settings of 255:255:12 and 36:72:12 from Section 4.2 as the attack configurations. Across all these attacks upon CIFAR10, 10% of the samples from the target class (representing 1% of the total samples) are poisoned, with the first class ("airplane") designated as the target class. We use the same evaluation metric mentioned in Section 4.2.1.

Attack Setup on CIFAR-100.(todo) For BadNets, a 33 checkerboard pattern is utilized as the trigger. For the Blended attack, a Hello-Kitty image is selected as the trigger and blended with the original images, with a transparency parameter of 0.2. Across all these attacks, 10% of the samples from the target class (representing 1% of the total samples) are poisoned, with the first class ("airplane") designated as the target class.

4.3.2 Result Analysis.

Method			*Metric*	*Attack*			
Type	no.	Selection		Badnets-C	Blended-C	255:255:12	36:72:12
Benchmark	a	Vanilla	BA	94.42%	94.90%	94.51%	94.95%
			ASR	37.24%	53.41%	1.37%	1.16%
	b	Loss Value	BA	94.71%	**95.10%**	94.84%	94.76%
			ASR	52.71%	59.43%	28.02%	47.85%
	c	Gradient Norm	BA	94.45%	94.77%	**95.04%**	**95.03%**
			ASR	52.56%	58.45%	38.26%	53.28%
	d	Forgetting Event	BA	**94.90%**	94.55%	94.92%	94.90%
			ASR	**71.74%**	**71.05%**	**74.39%**	**78.10%**
Our Method	e	Res-log	BA	**94.98%**	94.73%	94.54%	94.82%
			ASR	**82.13%**	82.34%	77.10%	80.20%
	f	Res-linear	BA	94.71%	94.31%	94.21%	94.63%
			ASR	68.65%	82.31%	76.73%	83.07%
	g	Res-square	BA	94.94%	94.38%	94.58%	94.59%
			ASR	78.76%	**84.88%**	**82.54%**	**83.88%**
	h	Res-exp	BA	94.47%	**94.80%**	**94.72%**	**94.85%**
			ASR	76.50%	71.81%	53.92%	62.28%

Table 2: Performance of attacks by poisoning 1% samples of CIFAR10. **Red** represents the negative performance of attacks. $N_p^R : N_p^G : N_p^B$ in **Method** of MultiBpp represents the concrete quantization setting of poisoning intensity in RGB channels.

Analysis on CIFAR10 From the comparison between images e, f, g and b, c, d, it can be concluded that incorporating considerations of category diversity in data filtering can significantly enhance attack effectiveness. Specifically, for BadNets attacks, our method, res-log, outperforms the currently best-performing forgetting event metric by 11 percentage points in Attack Success Rate (ASR), corresponding to 71.74% and 82.13%, respectively. For Blend attacks, our method exceeds the forgetting event metric by approximately 14 percentage points in ASR, corresponding to 71.05% and 84.88%, respectively. Regarding the newly proposed multi-bpp method in this paper, there is also an ASR improvement of over 6 percentage points.

The selection criteria for e-h are designed to incorporate considerations of category diversity from a light to a heavy degree. From the comparison between d and h across various attacks, it can be seen that excessively emphasizing category diversity is not the optimal strategy. Particularly for attack methods where the poisoning region covers the entire image (Blended-C, MultiBpp), the consideration of category diversity has a greater impact on the filtering strategy. The attack can

achieve the optimal combination of poisoned data under the more aggressive strategy g. However, excessively emphasizing category diversity can also lead to a greater decrease in Attack Success Rate (ASR). It is worth noting that BadNets attacks belong to the type of attacks that poison specific regions of images. Therefore, the learning of trigger features relies more on whether the samples themselves are difficult to learn, and thus considerations of category diversity should be introduced to a lesser extent. The attack can achieve the optimal combination of poisoned data under the less aggressive strategy e. Therefore, the choice of data filtering strategy needs to take into account the characteristics of the trigger itself. By reasonably designing a filtering strategy that incorporates considerations of category diversity based on the trigger characteristics, an optimal set of poisoned data can be obtained.

Method			*Metric*	*Poisoning Rate* $\alpha = 0.1\%$		*Poisoning Rate* $\alpha = 0.2\%$	
Type	no.	Selection		Badnets-C	Blended-C	Badnets-C	Blended-C
Benchmark	a	Vanilla	BA	94.42%	94.90%	94.51%	94.95%
			ASR	37.24%	53.41%	1.37%	1.16%
	b	Loss Value	BA	94.71%	**95.10%**	94.84%	94.76%
			ASR	52.71%	59.43%	28.02%	47.85%
	c	Gradient Norm	BA	94.45%	94.77%	**95.04%**	**95.03%**
			ASR	52.56%	58.45%	38.26%	53.28%
	d	Forgetting Event	BA	**94.90%**	94.55%	94.92%	94.90%
			ASR	**71.74%**	**71.05%**	**74.39%**	**78.10%**
Our Method	e	Res-log	BA	**94.98%**	94.73%	94.54%	94.82%
			ASR	**82.13%**	82.34%	77.10%	80.20%
	f	Res-linear	BA	94.71%	94.31%	94.21%	94.63%
			ASR	68.65%	82.31%	76.73%	83.07%
	g	Res-square	BA	94.94%	94.38%	94.58%	94.59%
			ASR	78.76%	**84.88%**	**82.54%**	**83.88%**
	h	Res-exp	BA	94.47%	**94.80%**	**94.72%**	**94.85%**
			ASR	76.50%	71.81%	53.92%	62.28%

Table 3: Performance of attacks upon CIFAR100.

Analysis on CIFAR100

4.4 Ablation Study

5 Conclusion

References

Jiawang Bai, Kuofeng Gao, Dihong Gong, Shu-Tao Xia, Zhifeng Li, and Wei Liu. Hardly perceptible trojan attack against neural networks with bit flips. In *European Conference on Computer Vision*, pages 104–121. Springer, 2022.

Peng Chen, Jirui Yang, Junxiong Lin, Zhihui Lu, Qiang Duan, and Hongfeng Chai. A practical clean-label backdoor attack with limited information in vertical federated learning. In *2023 IEEE International Conference on Data Mining (ICDM)*, pages 41–50. IEEE, 2023.

Xinyun Chen, Chang Liu, Bo Li, Kimberly Lu, and Dawn Song. Targeted backdoor attacks on deep learning systems using data poisoning. *arXiv preprint arXiv:1712.05526*, 2017.

Sheng-Yen Chou, Pin-Yu Chen, and Tsung-Yi Ho. Villandiffusion: A unified backdoor attack framework for diffusion models. *Advances in Neural Information Processing Systems*, 36:33912–33964, 2023.

Khoa Doan, Yingjie Lao, and Ping Li. Backdoor attack with imperceptible input and latent modification. *Advances in Neural Information Processing Systems*, 34:18944–18957, 2021.

Yinghua Gao, Yiming Li, Linghui Zhu, Dongxian Wu, Yong Jiang, and Shu-Tao Xia. Not all samples are born equal: Towards effective clean-label backdoor attacks. *Pattern Recognition*, 139:109512, 2023.

Yinghua Gao, Yiming Li, Xueluan Gong, Zhifeng Li, Shu-Tao Xia, and Qian Wang. Backdoor attack with sparse and invisible trigger. *IEEE Transactions on Information Forensics and Security*, 2024.

Tianyu Gu, Brendan Dolan-Gavitt, and Siddharth Garg. Badnets: Identifying vulnerabilities in the machine learning model supply chain. *arXiv preprint arXiv:1708.06733*, 2017.

Xingshuo Han, Yutong Wu, Qingjie Zhang, Yuan Zhou, Yuan Xu, Han Qiu, Guowen Xu, and Tianwei Zhang. Backdooring multimodal learning. In *2024 IEEE Symposium on Security and Privacy (SP)*, pages 3385–3403. IEEE, 2024.

Jonathan Hayase and Sewoong Oh. Few-shot backdoor attacks via neural tangent kernels. *arXiv preprint arXiv:2210.05929*, 2022.

Kaiming He, Xiangyu Zhang, Shaoqing Ren, and Jian Sun. Deep residual learning for image recognition. In *Proceedings of the IEEE conference on computer vision and pattern recognition*, pages 770–778, 2016.

Zirui Huang, Yunlong Mao, and Sheng Zhong. {UBA-Inf}: Unlearning activated backdoor attack with {Influence-Driven} camouflage. In *33rd USENIX Security Symposium (USENIX Security 24)*, pages 4211–4228, 2024.

Nguyen Hung-Quang, Ngoc-Hieu Nguyen, Thanh Nguyen-Tang, Kok-Seng Wong, Hoang Thanh-Tung, Khoa D Doan, et al. Wicked oddities: Selectively poisoning for effective clean-label backdoor attacks. In *The Thirteenth International Conference on Learning Representations*.

Tran Huynh, Dang Nguyen, Tung Pham, and Anh Tran. Combat: Alternated training for effective clean-label backdoor attacks. In *Proceedings of the AAAI Conference on Artificial Intelligence*, volume 38, pages 2436–2444, 2024.

Alaa Khaddaj, Guillaume Leclerc, Aleksandar Makelov, Kristian Georgiev, Hadi Salman, Andrew Ilyas, and Aleksander Madry. Rethinking backdoor attacks. In *International Conference on Machine Learning*, pages 16216–16236. PMLR, 2023.

Alex Krizhevsky, Geoffrey Hinton, et al. Learning multiple layers of features from tiny images. 2009.

Edwin H Land and John J McCann. Lightness and retinex theory. *Journal of the Optical society of America*, 61(1):1–11, 1971.

Haoyang Li, Qingqing Ye, Haibo Hu, Jin Li, Leixia Wang, Chengfang Fang, and Jie Shi. 3dfed: Adaptive and extensible framework for covert backdoor attack in federated learning. In *2023 IEEE Symposium on Security and Privacy (SP)*, pages 1893–1907. IEEE, 2023a.

Sen Li, Junchi Ma, and Minhao Cheng. Invisible backdoor attacks on diffusion models. *arXiv preprint arXiv:2406.00816*, 2024a.

Ziqiang Li, Pengfei Xia, Hong Sun, Yueqi Zeng, Wei Zhang, and Bin Li. Explore the effect of data selection on poison efficiency in backdoor attacks. *arXiv preprint arXiv:2310.09744*, 2023b.

Ziqiang Li, Hong Sun, Pengfei Xia, Beihao Xia, Xue Rui, Wei Zhang, Qinglang Guo, Zhangjie Fu, and Bin Li. A proxy attack-free strategy for practically improving the poisoning efficiency in backdoor attacks. *IEEE Transactions on Information Forensics and Security*, 2024b.

Junyu Lin, Lei Xu, Yingqi Liu, and Xiangyu Zhang. Composite backdoor attack for deep neural network by mixing existing benign features. In *Proceedings of the 2020 ACM SIGSAC conference on computer and communications security*, pages 113–131, 2020.

Yugeng Liu, Zheng Li, Michael Backes, Yun Shen, and Yang Zhang. Backdoor attacks against dataset distillation. *arXiv preprint arXiv:2301.01197*, 2023.

Peizhuo Lv, Chang Yue, Ruigang Liang, Yunfei Yang, Shengzhi Zhang, Hualong Ma, and Kai Chen. A data-free backdoor injection approach in neural networks. In *32nd USENIX Security Symposium (USENIX Security 23)*, pages 2671–2688, Anaheim, CA, August 2023. USENIX Association. ISBN 978-1-939133-37-3. URL `https://www.usenix.org/conference/usenixsecurity23/presentation/lv`.

Xiangyu Qi, Tinghao Xie, Ruizhe Pan, Jifeng Zhu, Yong Yang, and Kai Bu. Towards practical deployment-stage backdoor attack on deep neural networks. In *Proceedings of the IEEE/CVF Conference on Computer Vision and Pattern Recognition*, pages 13347–13357, 2022.

Filip Radenovic, Abhimanyu Dubey, and Dhruv Mahajan. Neural basis models for interpretability. *Advances in Neural Information Processing Systems*, 35:8414–8426, 2022.

Tianshi Wang, Fengling Li, Lei Zhu, Jingjing Li, Zheng Zhang, and Heng Tao Shen. Invisible black-box backdoor attack against deep cross-modal hashing retrieval. *ACM Transactions on Information Systems*, 42(4):1–27, 2024.

Xutong Wang, Yun Feng, Bingsheng Bi, Yaqin Cao, Ze Jin, Xinyu Liu, Yuling Liu, and Yunpeng Li. Not all benignware are alike: Enhancing clean-label attacks on malware classifiers. In *THE WEB CONFERENCE 2025*.

Zhenting Wang, Juan Zhai, and Shiqing Ma. Bppattack: Stealthy and efficient trojan attacks against deep neural networks via image quantization and contrastive adversarial learning. In *Proceedings of the IEEE/CVF conference on computer vision and pattern recognition*, pages 15074–15084, 2022.

Emily Wenger, Roma Bhattacharjee, Arjun Nitin Bhagoji, Josephine Passananti, Emilio Andere, Heather Zheng, and Ben Zhao. Finding naturally occurring physical backdoors in image datasets. *Advances in Neural Information Processing Systems*, 35:22103–22116, 2022.

Yutong Wu, Xingshuo Han, Han Qiu, and Tianwei Zhang. Computation and data efficient backdoor attacks. In *Proceedings of the IEEE/CVF International Conference on Computer Vision*, pages 4805–4814, 2023.

Yuan Xun, Xiaojun Jia, Jindong Gu, Xinwei Liu, Qing Guo, and Xiaochun Cao. Minimalism is king! high-frequency energy-based screening for data-efficient backdoor attacks. *IEEE Transactions on Information Forensics and Security*, 2024.

Yi Zeng, Minzhou Pan, Hoang Anh Just, Lingjuan Lyu, Meikang Qiu, and Ruoxi Jia. Narcissus: A practical clean-label backdoor attack with limited information. In *Proceedings of the 2023 ACM SIGSAC Conference on Computer and Communications Security*, CCS '23, page 771–785, New York, NY, USA, 2023. Association for Computing Machinery. ISBN 9798400700507. doi: 10.1145/3576915.3616617. URL `https://doi.org/10.1145/3576915.3616617`.

Shuai Zhao, Luu Anh Tuan, Jie Fu, Jinming Wen, and Weiqi Luo. Exploring clean label backdoor attacks and defense in language models. *IEEE/ACM Transactions on Audio, Speech, and Language Processing*, 2024.

Zihao Zhu, Mingda Zhang, Shaokui Wei, Li Shen, Yanbo Fan, and Baoyuan Wu. Boosting backdoor attack with a learnable poisoning sample selection strategy. *arXiv preprint arXiv:2307.07328*, 2023.

Algorithm 3 Metric Calculation with Negative Function N_F at $O(n)$

Input : Train Dataset D_{tr}, Target Label y_t, Misclassification Events $N_e((x_i, y_i), y_m)$
Output : Calculated Metric of Samples
for image $(x_i, y_t) \in D_{tr}$ **do**
  $Num[y_m], Sum = 0$
  for $y_m \in Y$ **do**
    $Num[y_m] = Num[y_m] + N_e((x_i, y_t), y_m)$
    $Sum = Sum + Num[y_m]$
  end for
end for
for $y_m \in Y$ **do**
  $Cls[y_m] = 1 - \frac{Num[y_m]}{Sum}$
end for
for image $(x_i, y_t) \in D_{tr}$ **do**
  $Metric[x_i] = 0$

for $y_m \in Y$ **do**
$Metric[x_i] = Metric[x_i] + Cls[y_m] * N_e((x_i, y_t), y_m)$
end for
end for

Algorithm 4 Metric Calculation with Negative Function N_F at $O(n^2)$

Input : Train Dataset D_{tr}, Target Label y_t, Misclassification Events $N_e((x_i, y_i), y_m)$
Output : Calculated Metric of Samples
for image $(x_i, y_t) \in D_{tr}$ **do**
$Num[y_m] = 0$
for $y_m \in Y$ **do**
$Num[y_m] = Num[y_m] + N_e((x_i, y_t), y_m)$
end for
end for
for $y_m \in Y$ **do**
$Sum = Sum + Num[y_m] * Num[y_m]$
end for
for $y_m \in Y$ **do**
$Cls[y_m] = 1 - \frac{Num[y_m] * Num[y_m]}{Sum}$
end for
for image $(x_i, y_t) \in D_{tr}$ **do**
$Metric[x_i] = 0$
for $y_m \in Y$ **do**
$Metric[x_i] = Metric[x_i] + Cls[y_m] * N_e((x_i, y_t), y_m)$
end for
end for

Algorithm 5 Metric Calculation with Negative Function N_F at $O(e^n)$

Input : Train Dataset D_{tr}, Target Label y_t, Misclassification Events $N_e((x_i, y_i), y_m)$
Output : Calculated Metric of Samples
for image $(x_i, y_t) \in D_{tr}$ **do**
$Num[y_m] = 0$
for $y_m \in Y$ **do**
$Num[y_m] = Num[y_m] + N_e((x_i, y_t), y_m)$
end for
end for
for $y_m \in Y$ **do**
$Sum = Sum + exp(-Num[y_m])$
end for
for $y_m \in Y$ **do**
$Cls[y_m] = 1 - \frac{exp(-Num[y_m])}{Sum}$
end for
for image $(x_i, y_t) \in D_{tr}$ **do**
$Metric[x_i] = 0$
for $y_m \in Y$ **do**
$Metric[x_i] = Metric[x_i] + Cls[y_m] * N_e((x_i, y_t), y_m)$
end for
end for